Title
Compensation of polarization-dependent loss in transmission fiber gratings by use of a Sagnac loop interferometer.

Journal
Optics letters, 30(1)

ISSN
0146-9592

Authors
Kim, Chang-Seok
Choi, Bernard
Nelson, J Stuart
et al.

Publication Date
2005

DOI
10.1364/ol.30.000020

Compensation of polarization-dependent loss in transmission fiber gratings by use of a Sagnac loop interferometer

Chang-Seok Kim, Bernard Choi, and J. Stuart Nelson

Beckman Laser Institute, University of California, Irvine, Irvine, California 92612

Qun Li, Pedram Zare Dashti, and H. P. Lee

Department of Electrical and Computer Engineering, Henry Samueli School of Engineering, University of California, Irvine, Irvine, California 92697

Received August 2, 2004

We analyze the transmission characteristics of a Sagnac loop interferometer containing a polarization-dependent loss element and lossless polarization-converting elements by use of Jones matrices. We show that polarization independence in the transmission mode can be achieved in such a configuration and that maximum transmittance occurs when a half-wave plate is used for the polarization-converting element. The result is verified experimentally for a fiber acousto-optic tunable filter and cascaded long-period fiber gratings with either intrinsic or process-induced polarization-dependent filtering characteristics. © 2005 Optical Society of America

OCIS codes: 060.2340, 230.5440, 120.5790.

Polarization-related effects such as polarization-dependent loss (PDL) and polarization mode dispersion are a major source of transmission impairment in optical fiber communication, sensors, measurement, and biomedical diagnostics.[1–3] For narrowband filters and high-resolution gratings, the polarization effect can lead to a polarization mode splitting of the filtering spectrum and grating response that severely hampers their performance. In fiber gratings the polarization effect can be intrinsic or process induced. For example, in microbending-induced long-period fiber gratings (LPFGs) the polarization effect originates from the polarization-dependent mode coupling between core and asymmetrical cladding modes,[3,4] whereas in UV- or CO_2-laser-exposed LPFGs[5,6] and fiber Bragg gratings[7] (FBGs) the polarization effect is caused by core mode birefringence introduced during the exposure process. Until now, to our knowledge, there has been no universal means of compensating for the polarization effect in fiber gratings. Polarization diversity or scrambling schemes are thought to be the only feasible means for alleviating this shortcoming. In this Letter we investigate a PDL compensation scheme by inserting a bidirectional PDL element inside an all-fiber Sagnac loop interferometer. Taking advantage of the polarization independence of the Sagnac interferometer for the transmitted port, with the aid of a polarization-converting element[8] we show that PDL can be eliminated for transmission fiber gratings. Since an all-fiber Sagnac interferometer can be easily constructed and can be wholly integrated with all-fiber devices, the new method alleviates a major hindrance for a number of all-fiber grating devices.

We first consider a bidirectional optical element with PDL as shown in Fig. 1(a). Assuming that the principal loss axes for the element are along the x and y axes (laboratory coordinates) and that there is no reflection, the propagation through this element can be described by Jones matrix

$$[J_p] = \begin{bmatrix} \alpha(\lambda)\exp[-j\phi_1(\lambda)] & 0 \\ 0 & \beta(\lambda)\exp[-j\phi_2(\lambda)] \end{bmatrix},$$

where $\alpha(\lambda)$ and $\beta(\lambda)$ and $\phi_1(\lambda)$ and $\phi_2(\lambda)$ are the transmission and phase factors for the x- and y-polarized electric fields at λ, respectively. For an input field $E_{\text{in}} = [E_x \quad E_y\exp(j\varphi)]^T$, where E_x and E_y are the electric field amplitudes in the x and y directions, respectively, and φ is the phase delay between them, the corresponding transmitted output intensity is $I_{\text{out}}(\lambda) = \alpha(\lambda)^2 |E_x|^2 + \beta(\lambda)^2 |E_y|^2$, which is clearly polarization dependent. The result holds for propagation in both directions.

Next, we consider the transmittance when the PDL element is placed inside a Sagnac interferometer with two polarization-converting elements A and B (described by two unitary Jones matrices:

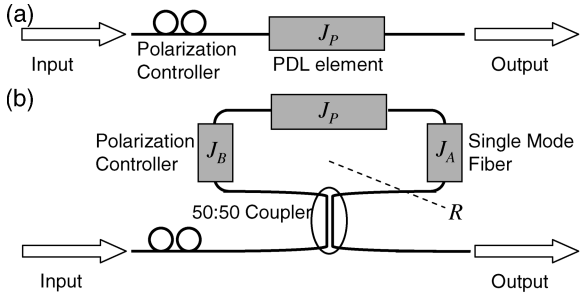

Fig. 1. Schematic of the PDL element placed (a) outside and (b) inside a Sagnac interferometer containing two polarization-converting elements, A and B. The effect of the folded fiber inside the Sagnac loop is represented by matrix R as labeled in the figure.

0146-9592/05/010020-03$15.00/0

$$[J_A] = \begin{bmatrix} A & -B^* \\ B & A^* \end{bmatrix}, \qquad [J_B] = \begin{bmatrix} C & -D^* \\ D & C^* \end{bmatrix},$$

where $|A|^2 + |B|^2 = |C|^2 + |D|^2 = 1$) on either side of the PDL element, which take into account single-mode fiber (SMF) and (or) wave plates present on each side, as shown in Fig. 1(b). The case for a lossless element was previously analyzed in Ref. 9. Following a procedure similar to Ref. 9, transmission matrix $[T(\lambda)]$ and transmitted output intensity $I_{\text{out}}(\lambda)$ can be expressed as

$$\begin{aligned}[T(\lambda)] &= [K_\parallel][R][J_A][J_P][J_B][K_\parallel] \\ &\quad + [K_X][J_B]^T[J_P]^T[J_A]^T[R][K_X] \\ &= t_s(\lambda)\begin{bmatrix} 0 & 1 \\ -1 & 0 \end{bmatrix}, \end{aligned} \tag{1}$$

$$I_{\text{out}}(\lambda) = |t_s(\lambda)|^2(|E_x|^2 + |E_y|^2), \tag{2}$$

where $[R]$ is a coordinate-conversion matrix for the folded fiber loop inside the Sagnac interferometer and $[K_\parallel]$ and $[K_X]$ are the parallel-coupling and cross-coupling matrices, respectively, for the 2×2 fiber coupler. These matrices are given as

$$[R] = \begin{bmatrix} -1 & 0 \\ 0 & 1 \end{bmatrix},$$

$$[K_\parallel] = \begin{bmatrix} (1-k_x)^{1/2} & 0 \\ 0 & (1-k_y)^{1/2} \end{bmatrix},$$

$$[K_X] = \begin{bmatrix} j(k_x)^{1/2} & 0 \\ 0 & j(k_y)^{1/2} \end{bmatrix},$$

where k_x and k_y are the power-coupling coefficients for the x and y polarizations, respectively. For a polarization-independent lossless 50:50 coupler, $k_x = k_y = k = 0.5$, and t_s is given by

$$\begin{aligned} t_s(\lambda) = \frac{1}{2}\{&[\alpha(\lambda)\exp(-j\phi_1)](AD^* - BC) \\ &+ [\beta(\lambda)\exp(-j\phi_2)](B^*C^* - A^*D)\}. \end{aligned}$$

Equation (2) shows that $I_{\text{out}}(\lambda)$ in a Sagnac interferometer is polarization independent. The only conditions under which polarization independence will hold are that both matrices $[J_A]$ and $[J_B]$ are unitary. Null transmission occurs when both $[J_A]$ and $[J_B]$ are unity matrices, which corresponds to a loop mirror containing a PDL element. Although we assumed that the principal loss axes for the PDL element lie in the x and y directions, the proof holds when the loss axes are oriented at an arbitrary angle relative to the laboratory coordinates.

The simplest way to implement a Sagnac interferometer is to replace $[J_A]$ with a section of SMF with negligible birefringence and $[J_B]$ with a polarization controller (PC); that is, replace $[J_A]$ and $[J_B]$ with

$$\begin{bmatrix} 1 & 0 \\ 0 & 1 \end{bmatrix}, \qquad \begin{bmatrix} \cos\theta & -\sin\theta \\ \sin\theta & \cos\theta \end{bmatrix}$$

$$\times \begin{bmatrix} \exp[i\Gamma(\lambda)/2] & 0 \\ 0 & \exp[-i\Gamma(\lambda)/2] \end{bmatrix} \begin{bmatrix} \cos\theta & \sin\theta \\ -\sin\theta & \cos\theta \end{bmatrix},$$

respectively, where Γ is the retardance and θ is the orientation of the axes of the wave plate with respect to the laboratory coordinates.

Under this condition and assuming that $\phi_1(\lambda) \approx \phi_2(\lambda)$, transmittance $T(\lambda)$ becomes

$$T(\lambda) = \frac{1}{4}[\alpha(\lambda) + \beta(\lambda)]^2 \sin^2\frac{\Gamma(\lambda)}{2}\sin^2 2\theta. \tag{3}$$

From Eq. (3), maximum transmittance $T_{\max}(\lambda)$ is equal to $[\alpha(\lambda) + \beta(\lambda)]^2/4$ and can be attained when $\theta = \pi/4$ and $\Gamma(\lambda) = \pi$, that is, when the PC functions as a half-wave plate. Minimum transmittance $T_{\min}(\lambda)$ is zero when either Γ or θ is 0.

To verify the above-described PDL compensation scheme, we examined the polarization dependence of a fiber acousto-optic tunable filter (AOTF) placed inside and outside the Sagnac interferometer.[9] Similarly to a microbending LPFG, in a flexural-wave-induced fiber AOTF, only asymmetrical cladding modes (hybrid LP_{1n} modes) are excited because of the asymmetrical index perturbation profile. The LP_{1n} modes consist of several nearly degenerate constituent modes (TE_{0n}, TM_{0n}, and HE_{2n}). These modes have different polarization-dependent coupling strengths. Owing to their different propagation constants (β), the individual resonant wavelengths are slightly different, but their linewidths overlap. This leads to a polarization mode splitting effect in which the maximum wavelength of the filtering spectrum shifts with the input state of polarization (SOP). This shift is of the order of 0.1–0.15 nm for conventional step-index SMF.[3]

To accentuate the polarization mode splitting, we etch down the fiber cladding, which is known to increase the spectral separation of β among the constituent LP_{1n} cladding modes.[10] In the present work, the length and etched diameter of the bare SMF are 10 cm and 40 μm, respectively, and the operating acoustic frequency is 1940 kHz. The transmission spectra are measured with a polarized broadband light source and an optical spectrum analyzer with 0.1-nm resolution. The PC inside the loop is adjusted to achieve maximum transmission, and the results are shown in Fig. 2. The dashed curves in Fig. 2(a) correspond to the transmission spectra at two extreme input SOPs I and II that yield the widest spectral separation when the fiber AOTF is placed outside the Sagnac interferometer. The filtering spectra become nearly polarization independent when the fiber AOTF is inserted inside the Sagnac interferometer as shown by the solid curves in Fig. 2(a). Figure 2(b) also shows the corresponding PDL versus wavelength for each configuration based on the filtering spectra in

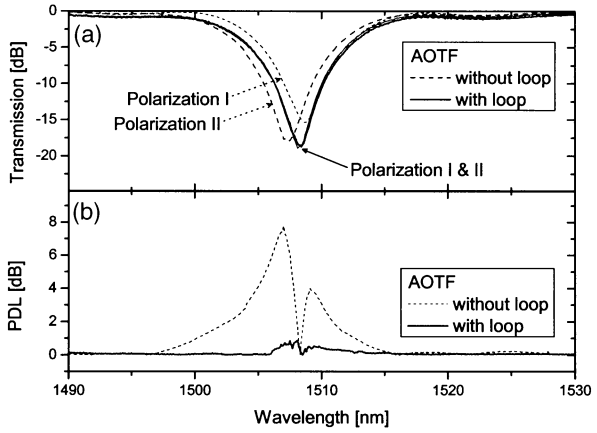

Fig. 2. (a) Transmission spectra of the fiber AOTF for various input SOPs when the AOTF is placed outside (dashed curves) and inside (solid curves) the Sagnac interferometer. (b) Corresponding PDL of the device described in (a) under the two placements.

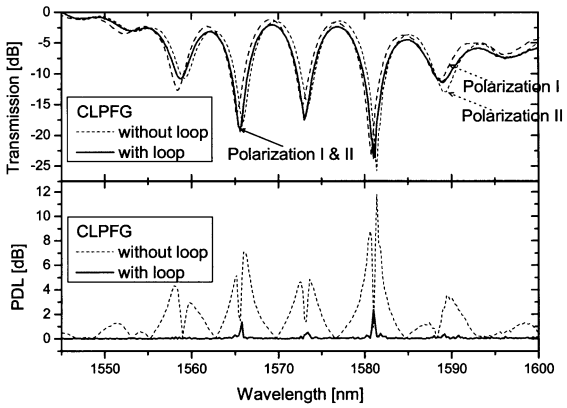

Fig. 3. (a) Transmission spectra of a cascaded two-stage LPFG (CLPFG) for various input SOPs when the CLPFG is placed outside (dashed curves) and inside (solid curve) the Sagnac interferometer. (b) Corresponding PDL of the device described in (a) under the two placements.

Fig. 2(a). The near elimination of the PDL (from 8 to <0.6 dB) of the fiber AOTF when the Sagnac interferometer is used is clearly evident. The residual PDL is probably caused by the imperfection of the 50:50 coupler and measurement noise.

We carry out our next PDL compensating experiment by measuring the transmission spectra of a cascaded two-stage LPFG comb filter placed inside and outside the Sagnac interferometer. The PDL of this LPFG device originates from the asymmetric profile of the refractive index in the fiber when the fiber is subjected to the single-sided exposure of UV laser radiation that results in the splitting of resonances from each of the two orthogonally polarized core modes.[5] This polarization effect is intensified when two LPFGs are cascaded together to form a high-finesse Mach–Zehnder interferometer comb filter. In this experiment the grating period and the total length of each LPFG are 400 μm and 2 cm, respectively, whereas the separation between the two LPFGs is 9 cm. The dashed curve in Fig. 3(a) shows the maximum spectral shift of the comb filter for two input SOPs. When the cascaded LPFG is inserted inside the Sagnac interferometer, the polarization-dependent spectral shift is largely eliminated, as shown by the solid curve in Fig. 3(a). The corresponding PDL versus wavelength is plotted in Fig. 3(b). The still rather large PDL ($\sim$2 dB) after compensation near the resonances of the comb filter is thought to be due to the noise level of the measurement, since the cascaded LPFG has a very narrow and steep spectral response.

Although we have demonstrated PDL compensation for fiber gratings inside an all-fiber Sagnac interferometer, the PDL compensating mechanism described here is wholly generic. It is conceivable that such a polarization compensation scheme can be applied to transmission-type integrated-optic and other guided-wave resonant structures such as spherical and toroid resonators[11] of both passive and active nature. The case for a reflection filter such as a FBG is more complicated because the interference paths have different lengths, giving rise to interference fringes that change the reflection spectrum of the original FBG.[12]

In summary, a new method for compensating PDL in transmission fiber gratings by use of a Sagnac loop interferometer has been described and verified on a flexural-wave-induced fiber AOTF and a cascaded two-section LPFG comb filter. The new method provides a useful means of addressing PDL impairment for transmission-type devices irrespective of the origin of their PDLs.

This work was supported in part by National Science Foundation grant 0330496; the Arnold and Mabel Beckman Fellows Program; and National Institutes of Health grants AR47551, AR48458, and EB002495.
C. S. Kim's e-mail address is cskim@laser.bli.uci.edu.

References

1. B. L. Bachim and T. K. Gaylord, Appl. Opt. **42,** 6816 (2003).
2. J. Zhang, S. G. Guo, W. G. Jung, J. S. Nelson, and Z. P. Chen, Opt. Express **11,** 3262 (2003), http://www.opticsexpress.org.
3. Q. Li, A. A. Au, C. H. Lin, I. V. Tomov, and H. P. Lee, IEEE Photon. Technol. Lett. **15,** 718 (2003).
4. H. S. Kim, S. H. Yun, I. K. Hwang, and B. Y. Kim, Opt. Lett. **22,** 1476 (1997).
5. B. Lee, J. Cheong, and U. C. Paek, Opt. Lett. **27,** 1096 (2002).
6. S. T. Oh, W. T. Han, U. C. Paek, and Y. Chung, Opt. Express **11,** 3087 (2003), http://www.opticsexpress.org.
7. S. Pereira, J. E. Sipe, R. E. Slusher, and S. Spalter, J. Opt. Soc. Am. B **19,** 1509 (2002).
8. C. S. Kim, F. N. Farokhrooz, and J. U. Kang, Opt. Lett. **29,** 1677 (2004).
9. A. Yu and A. S. Siddiqui, IEE Proc. Optoelectron. **141,** 1 (1994).
10. Q. Li, X. Liu, J. Peng, B. Zhou, E. R. Lyons, and H. P. Lee, IEEE Photon. Technol. Lett. **14,** 337 (2002).
11. K. Armani, T. J. Kippenberg, S. M. Spillane, and K. J. Vahala, Nature **421,** 925 (2003).
12. X. Shu, L. Yu, D. Zhao, L. Zhang, K. Sugden, and I. Bennion, J. Opt. Soc. Am. B **19,** 2770 (2002).